FOREX Publication
Open Access | Rapid and quality publishing

International Journal of
Electrical and Electronics Research (IJEER)
Case Study | Volume 14, Issue 01| Pages 10-17| e-ISSN: 2347-470X

Bandwidth-Enhanced Microstrip Patch Antenna Configurations for Sub-6 GHz and mmWave 5G Applications

Kolli.Venkatrao[1], and G. Merlin Sheeba[2]

[1]Research Scholar, School of Electrical and Electronics Engineering Sathyabama Institute of Science and Technology, Chennai, India; kolli.venkat436@gmail.com
[1]Assistant Professor Department of ECE, SRKR Engineering College, Bhimavaram, Andhra pradesh, India; kolli.venkat436@gmail.com
[2]Professor, Department of ECE, Jerusalem College of Engineering, Chennai, India: drmerlinsheebag@gmail.com

***Correspondence :** *Kolli Venkatrao, kolli.venkat436@gmail.com*

ABSTRACT- The evolution from 4G to 5G introduces several design challenges, including spectrum sharing, significantly wider operating bandwidths, and advanced antenna design. To meet the demands of 5G communication, antennas must exhibit compact geometry, an efficient and well-matched feeding mechanism, and compatibility with large-scale manufacturing. This paper presents the design and optimization of a microstrip antenna operating at the 28 GHz band. The proposed antenna undergoes iterative modifications, focusing on the feed line configuration and radiating patch geometry to enhance performance. At each stage, key performance metrics including S11, gain and radiation pattern are thoroughly evaluated. Furthermore, the impact of geometric irregularities introduced along the feed line plane on the antenna's resonant behavior, gain, and radiation profile is systematically investigated. All simulations and parametric studies are performed using ANSYS HFSS, and the antenna's overall performance is assessed based on the obtained electromagnetic simulation results.

Keywords: NR, 5G, MPA, VSWR and Tapering.

ARTICLE INFORMATION
Author(s): Kolli.Venkatrao and G.Merlin Sheeba;
Received: 09/09/25; **Accepted**: 19/01/26; **Published**: 10/03/26;
E- ISSN: 2347-470X.
Paper Id: IJEER250142
Citation: 10.37391/ijeer.140102
Webpage-link:
https://ijeer.forexjournal.co.in/archive/volume-14/ijeer-140102.html

Publisher's Note: FOREX Publication stays neutral with regard to jurisdictional claims in Published maps and institutional affiliations.

1. INTRODUCTION

The introduction of 4G technology in 2009 marked a pivotal advancement in wireless communication, delivering data rates nearly ten times faster than those of its 3G predecessor. This technological leap significantly influenced various sectors, including commercial, satellite, and defense communications. The commercial sector, in particular, experienced rapid advancements driven by the widespread adoption of the Internet of Things (IoT). Simultaneously, the emergence of Industry 4.0 highlighted the growing demand for high-speed, reliable, and robust connectivity capable of supporting next-generation industrial automation. With the advent of 5G, wireless communication has transitioned to much higher frequency bands, typically ranging from 28 GHz to 100 GHz, enabling data rates up to 10 Gbps [1-3]. According to the 3GPP New Radio (NR) standards, 5G networks are engineered to be intelligent, reliable, and highly efficient. However, the shift to higher frequencies introduces fundamental trade-off higher data rates result in broad coverage. To address this, technologies such as Enhanced Mobile Broadband (eMBB) have been developed to maintain high-speed performance across expansive areas. eMBB also facilitates low-latency, high-reliability networks crucial for mission-critical communications (CMC), including autonomous vehicles and remote surgical operations. Complementing eMBB, Ultra-Reliable Low Latency Communications (URLLC) provides dependable data transmission in environments with dense device connectivity. Additionally, massive Machine-Type Communication (mMTC), which effectively manages sporadic, high-volume data bursts in heavily connected environments. The adaptability and reconfigurability of system components, particularly antennas, are vital for accommodating the dynamic nature of 5G applications.

The advent of fifth generation (5G) wireless communication has introduced unprecedented demands for ultra-high data rates, massive device connectivity, and ultra-low latency [4-6]. To support these requirements, antenna systems must exhibit compact geometry, high gain, and wide bandwidth. Microstrip patch antennas (MPAs) are well-suited for 5G applications due to their low profile, lightweight structure, ease of fabrication and compatibility with planar and conformal surfaces [14-15]. However, conventional MPAs are limited by inherently narrow bandwidth limiting their performance in critical 5G frequency bands, particularly with in the sub-6 GHz and millimeter-wave ranges [7-9]. To overcome these limitations, numerous enhancement techniques have been proposed. Bandwidth improvement techniques include geometric modifications (*e.g.*, U-slots, fractal shapes, and DGS), advanced substrate engineering, innovative feeding methods, and the integration of additional elements such as parasitic structures and metamaterials [16]. Typically composed of a

FOREX Publication
Open Access | Rapid and quality publishing
International Journal of Electrical and Electronics Research (IJEER)
Case Study | Volume 14, Issue 01| Pages 10-17| e-ISSN: 2347-470X

radiating patch on a dielectric substrate over a ground plane, the performance of an MPA is influenced by patch geometry, substrate characteristics, and feeding mechanisms [17-18]. Despite their advantages, MPAs often exhibit fractional bandwidths of only 1–5%, necessitating further optimization for effective deployment in modern 5G systems.

Bandwidth enhancement in microstrip patch antennas can be achieved through several structural and EM techniques. Bandwidth can be enhanced by incorporating slots to alter surface current distribution, applying fractal designs to increase effective electrical length [19], and introducing defected ground structures (DGS) for better impedance matching [20]. Substrate optimization such as use of low-permittivity materials, stacked configurations, and electromagnetic bandgap (EBG) structures for further bandwidth enhancement [21]. Feeding techniques like proximity and aperture coupling reduce spurious emissions and improve impedance characteristics [22], while corporate feed networks ensure uniform power delivery in array systems [23]. Parasitic and artificial EM structures, including split-ring resonators (SRRs) and metamaterials with negative permittivity or permeability, have demonstrated significant bandwidth improvements [24–25]. For sub-6 GHz applications, techniques such as fractals, DGS and substrate stacking are widely employed [19–20], whereas millimeter-wave designs address challenges like propagation loss and fabrication tolerances using high-gain arrays, low-loss substrates, and beam-steering capabilities [18]. Empirical studies validate the efficacy of these techniques. For instance, integrating a U-slot improved the bandwidth of an MPA at 3.5 GHz from 2% to 12% [16], while dual-layer substrates achieved up to 25% bandwidth enhancement [20]. The inclusion of SRRs demonstrated fractional bandwidths as high as 15% [25–28]. Looking ahead, 5G-driven antenna developments include hybrid designs combining MPAs with dielectric resonator antennas (DRAs), additive manufacturing for complex geometries, machine learning-assisted optimization, and the development of eco-friendly materials [21]. These innovations are expected to play a critical role in achieving reliable, efficient, and sustainable next-generation wireless communication systems. In summary, the design of MPAs for 5G relies on a multi-faceted approach involving structural, material, and computational innovations to overcome inherent bandwidth limitations and meet the stringent performance requirements of emerging communication networks. In this context, microstrip patch antennas have emerged as promising candidates due to their low-profile planar structure, ease of fabrication, and suitability for miniaturization particularly in mobile and wearable devices. Their geometrical flexibility in design geometry allows for tailored performance to meet the stringent requirements of 5G systems. The remainder of this paper is structured as follows: *Section 2* presents the proposed antenna geometry. *Section 3* discusses the simulation methodology along with corresponding results and analysis. *Section 4* covers the fabrication and measured results of the prototype. Finally, *Section 5* concludes the paper with key insights and findings.

2. PROPOSED GEOMETRY

The proposed antenna design begins with a conventional microstrip rectangular patch geometry employing an edge-fed feeding technique. The fundamental mathematical analysis of the rectangular patch is considered from the reference [15]. The detailed geometrics of the proposed MPA is described sequentially as follows;

2.1. Geometry-1

The initial design configuration consists of rectangular-shaped radiating patch with dimensions of 5.5 mm width and 4.17 mm length is placed on a square-shaped roger Rogers 5880 substrate with dimension of 12mm^2 and the thickness of the substrate is 0.508 mm. The rectangular patch is excited using an edge-fed using a microstrip feed technique with a width of 0.45 mm and 6 mm long line extends from the centre of the one substrate edge to excite the patch.

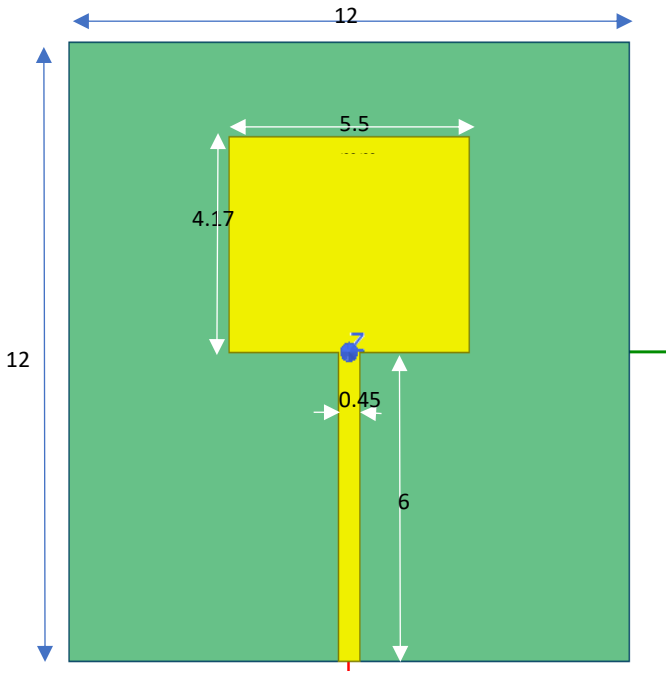

Figure 1. Basic Patch antenna

2.2. Geometry-2

Geometry-2 is developed as an evolution of Geometry-1 by introducing curvature along the edges of the rectangular radiating patch. Specifically, each corner is rounded using a circular arc of radius of 0.5 mm, resulting in a smoother boundary transition. This geometrical modification is aimed at influencing the current distribution across the radiating surface, which can potentially improve impedance matching and reduce edge diffraction effects. Importantly, no additional structural changes are introduced, the structure with the same substrate material, feed line configuration, and overall dimensions remain identical to those in Geometry-1. This approach isolates the effect of edge curvature, enabling a focused analysis of its impact on the antenna's performance metrics like S11, gain, and radiation pattern.

FOREX Publication
Open Access | Rapid and quality publishing
International Journal of Electrical and Electronics Research (IJEER)
Case Study | Volume 14, Issue 01| Pages 10-17| e-ISSN: 2347-470X

Figure 2. Corner truncated patch antenna

2.3. Geometry-3

Geometry-3 builds upon the structure of Geometry-2 by introducing significant refinement to the microstrip feed line. In this configuration, the uniform feed line is replaced with a tapered, non-uniform profile designed to improve impedance matching between the ML and the radiating patch. Specifically, the feed line starts with a width of 0.45 mm at the edge of the substrate and gradually narrows to 0.25 mm as it approaches the radiating patch. This gradual transition occurs over a length of 2 mm and is achieved in four uniform steps, each with a decrement of 0.05 mm at evenly spaced intervals of 0.5 mm. The tapering technique is strategically employed to minimize abrupt discontinuities along the transmission path, which can cause impedance mismatches and reflection losses. By creating a smoother transition from the feed line to the patch, the design helps ensure a better power transfer, thereby enhancing overall antenna performance. Importantly, all other structural parameters and substrate properties remain unchanged from Geometry-2. The modification in Geometry-3 is aimed at optimizing the return loss and improves bandwidth performance by minimizing reflections at the feed-point interface.

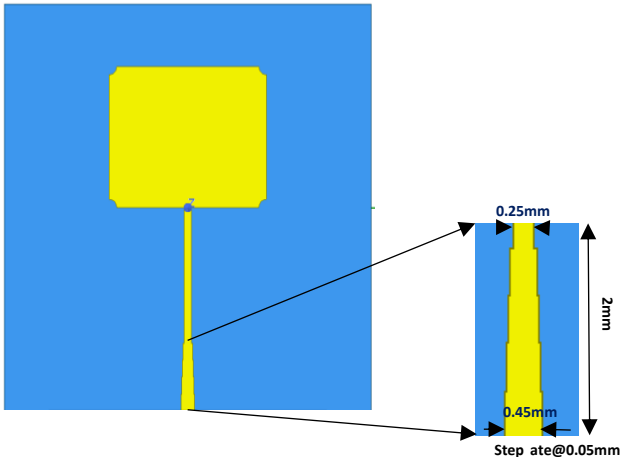

Figure 3. Modified feed truncated patch antenna

2.4. Geometry-4

Geometry-4 introduces a further refinement to the feed line structure by modifying both the width variation profile and the number of impedance transition steps employed in Geometry-3. Unlike the gradual four-step tapering used previously, Geometry-4 employs a more abrupt transition in the feed line width. Specifically, the microstrip feed line starts with a width of 0.4 mm at the edge of the substrate and undergoes a single-step reduction to 0.2 mm. This abrupt transition positioned approximately 2 mm from the substrate's edge, just before the feed line connects to the radiating patch. The motivation behind this modification is to evaluate the impact of an abrupt impedance transition on the antenna's return loss and matching performance. By reducing the number of transitions to one, the design aims to simplify the fabrication process while still maintaining acceptable electrical performance. All other parameters of the antenna, including the patch geometry and substrate characteristics, are preserved from the previous geometry to isolate the effect of the feed line variation.

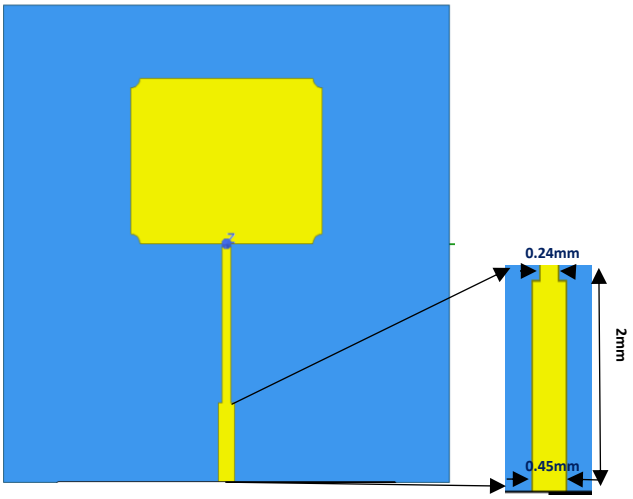

Figure 4. stepped line feed truncated patch antenna

2.5. Geometry-5

In Geometry-5, the feed line configuration undergoes an advanced modification by extending the non-uniform stepped variation along its entire length. This approach differs from Geometry-4, which utilized a single abrupt step and Geometry-3, where the stepped width variation was confined to the final 2 mm of the feed line. In Geometry-5, the feed line width is gradually tapered from the substrate edge to the patch connection point through multiple uniform steps distributed across its full 6 mm length. This extended tapering is designed to achieve a smoother impedance transition, leading to improved impedance matching and reduced reflection losses. By distributing the steps uniformly, the design enhances EM propagation from the source to the patch, potentially resulting in better return loss characteristics and radiation performance. All other antenna parameters, including the patch geometry and substrate properties, remain consistent to isolate the effect of the feed line modification.

FOREX Publication
Open Access | Rapid and quality publishing
International Journal of Electrical and Electronics Research (IJEER)
Case Study | Volume 14, Issue 01| Pages 10-17| e-ISSN: 2347-470X

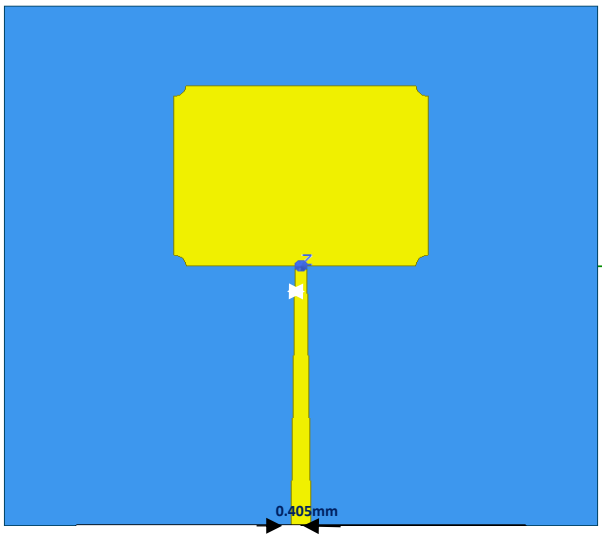

Figure 5. Proposed balun feed truncated patch antenna

3. RESULTS AND DISCUSSIONS

3.1. Case-1

This section presents the simulation results for the proposed antenna geometries. The performance analysis focuses on key radiation characteristics including S_{11}, VSWR and 3D radiation pattern. In the initial case, geometry-1 is evaluated and the corresponding simulation results are shown in *figures 6(a)-6(c)*. As observed from *figure 6(a)*, the antenna resonates at 28 GHz with a notably low S11. Additionally, the VSWR remains well below the acceptable threshold across the same frequency band, indicating good impedance matching. Based on these favourable parameters, the 3D radiation pattern for Geometry-1 is generated and illustrated in *figure 6(c)*.

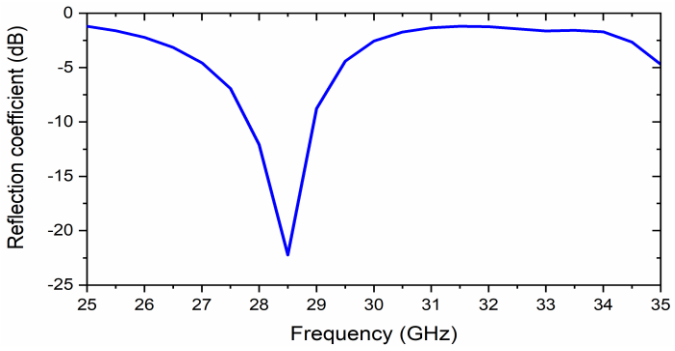

(a)

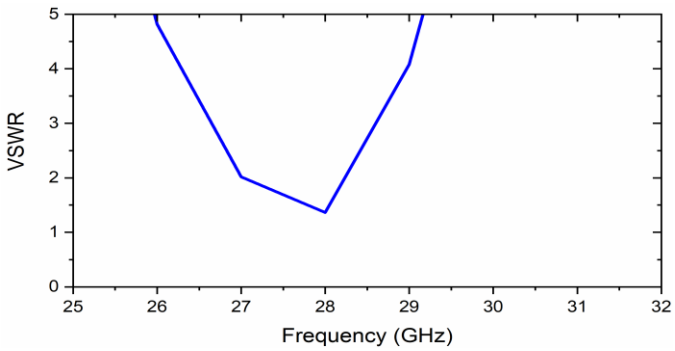

(b)

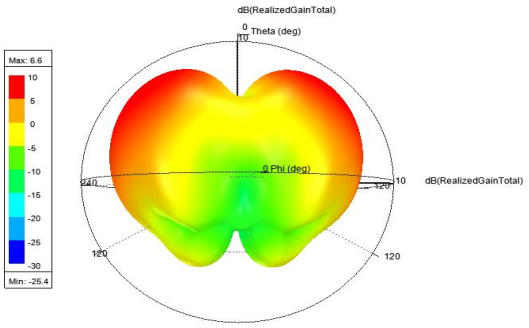

(c)

Figure 6. Characteristics of Geometry-1 a) Reflection coefficient (b) VSWR and (c) 3D pattern

3.2. Case-2

Based on the S11 and VSWR results, the antenna exhibits a resonant frequency at 28 GHz, and the corresponding radiation pattern for Geometry-2 confirms stable and consistent behavior at this frequency.

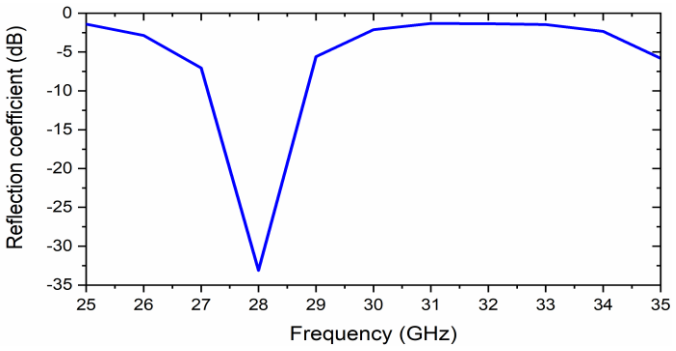

(a)

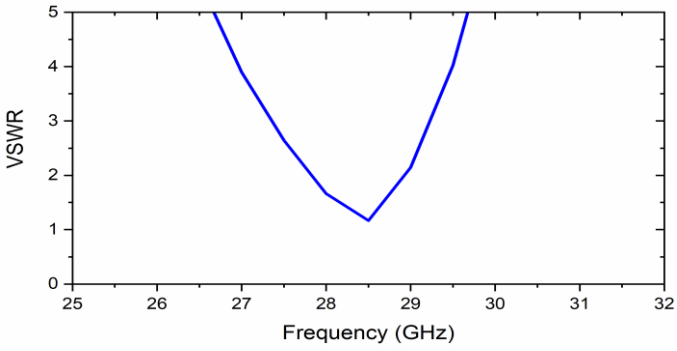

(b)

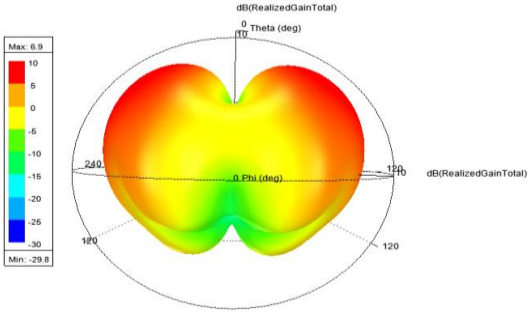

(c)

Figure 7. Characteristics of geometry-2 (a) S11 (b) VSWR and (c) Radiation Pattern

FOREX Publication
Open Access | Rapid and quality publishing
International Journal of Electrical and Electronics Research (IJEER)
Case Study | Volume 14, Issue 01| Pages 10-17| e-ISSN: 2347-470X

3.3. Case-3

The performance characteristics of Geometry-3 are illustrated in *figures 8(a)* through *8(c)*. Although it demonstrates radiation behavior similar to Geometries 1 and 2, notable variations are observed in the magnitudes of the reflection coefficient (S_{11}) and VSWR. The radiation pattern retains a consistent shape, characterized by two well-defined lobes that are clearly separated from each other.

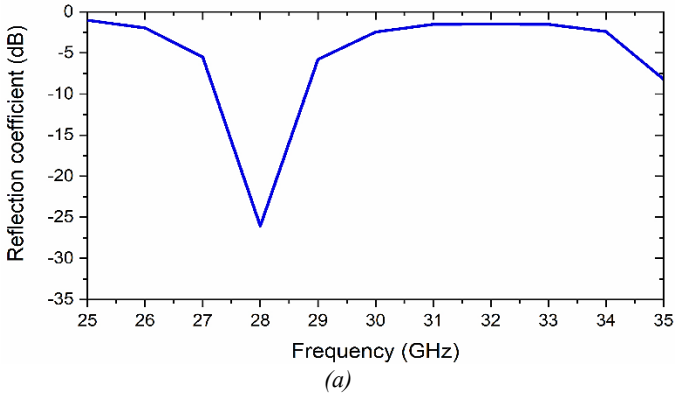

(a)

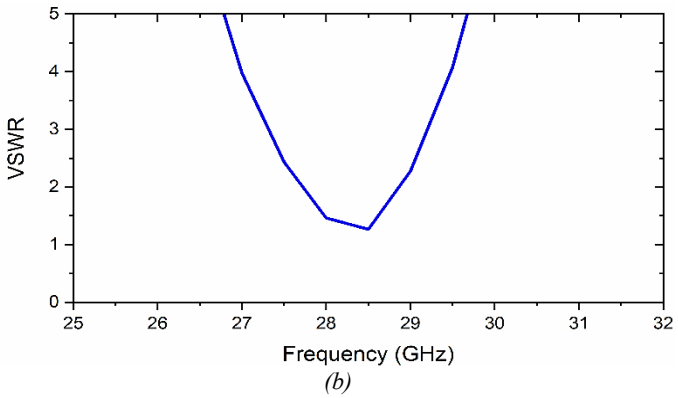

(b)

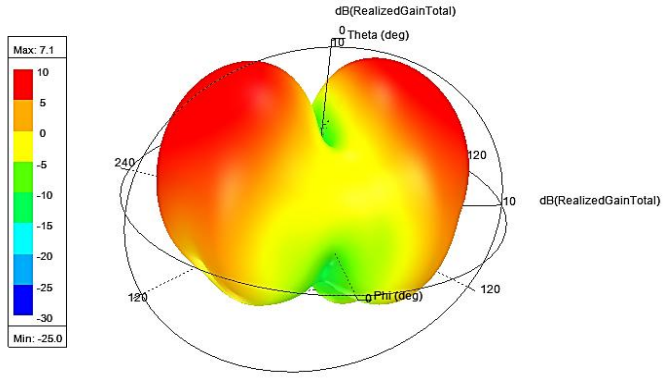

(c)

Figure 8. Characteristics of geometry-3 (a) S11 (b) VSWR and (c) Radiation Pattern

3.4. Case-4

Interestingly, the frequency response plots for Geometries 4 and 5, as illustrated in *figures 5* and *6*, exhibit nearly identical resonant frequencies. However, variations in magnitude can be attributed to differences in their respective feed-line geometries, which directly influence impedance matching and field distribution.

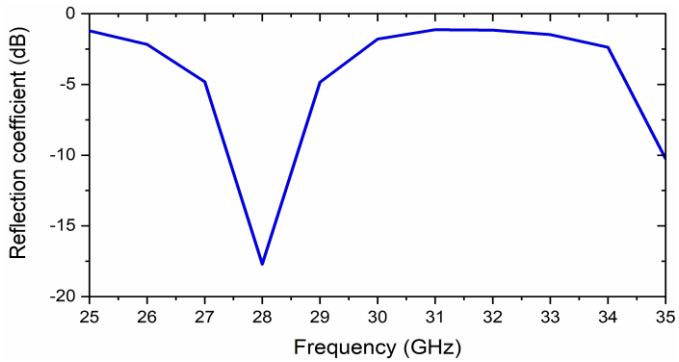

(a)

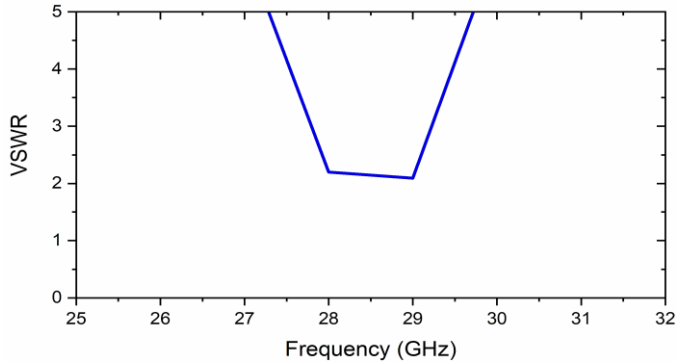

(b)

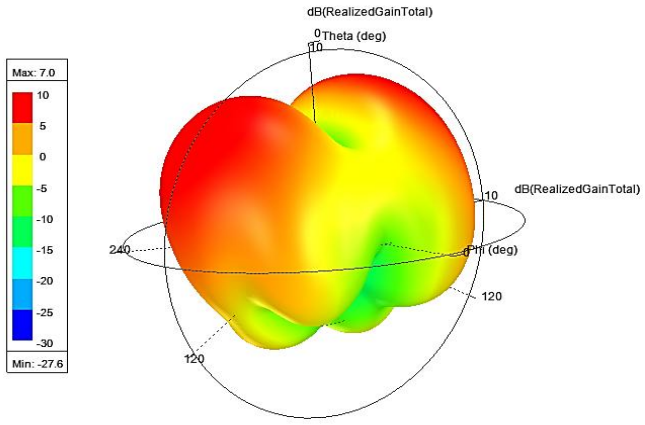

(c)

Figure 9. Characteristics of geometry-4 a) S11 (b) VSWR and (c) Radiation Pattern

3.5. Case-5

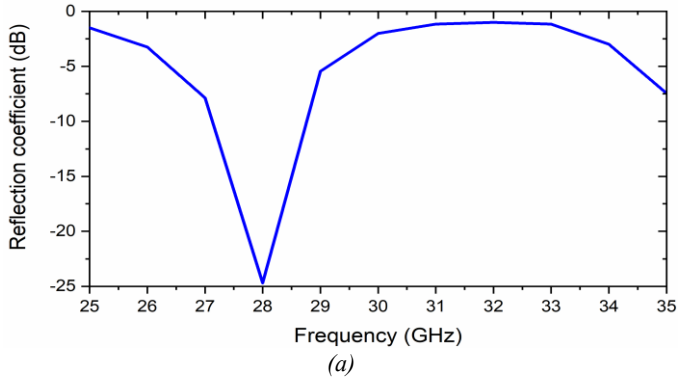

(a)

FOREX Publication
Open Access | Rapid and quality publishing
International Journal of Electrical and Electronics Research (IJEER)
Case Study | Volume 14, Issue 01| Pages 10-17| e-ISSN: 2347-470X

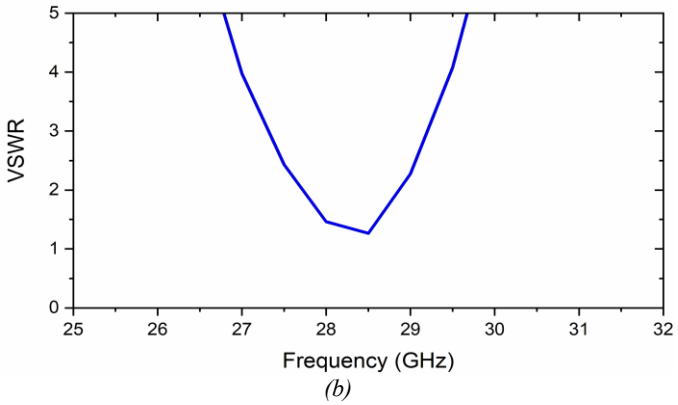

(b)

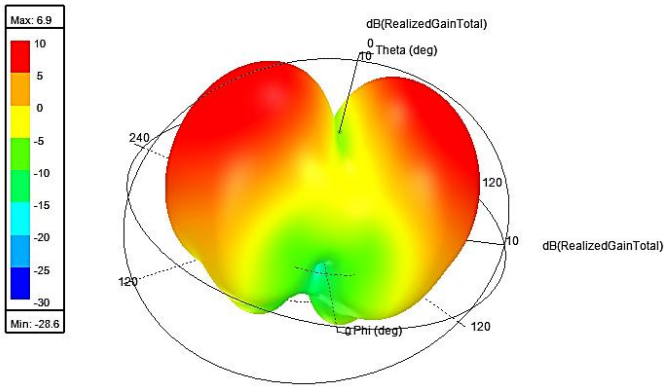

(c)

Figure 10. Characteristics of geometry-5 (a) S11 (b) VSWR and (c) Radiation Pattern

Table 1. Characteristics of different geometry

S. No.	Description	Return loss(dB)	Gain(dB)
1	Microstrip line (ML)	-24.69	6.6
2	ML with Circular etching slot on all the edges of the patch	-33.11	6.7
3	ML with a increment step size of 0.05mm from edge of the substrate to the edge of the patch. The step size changes from 0.45mm to 0.24mm	-26.06	6.8
4	ML with single step i.e., from step size 0.45mm to 0.24mm with Circular slot on edges of the patch	-17.70	7.0
5	ML with BALUN impedance transition ie. 0.45mm to 0.24mm with Circular slot on edges of the patch	-24.93	6.9

Table 1 summarizes the performance characteristics for all geometries. Although the resonant frequency and the 3D radiation patterns remain consistent across the configurations, significant variations in gain and return loss are evident, arising from the corresponding geometric modifications applied to each structure.

4. MEASURED RESULTS

The fabricated prototype of the BALUN-fed microstrip patch antenna, along with a comparison of simulated and measured performance is illustrated in *figure 7*. This figure includes two key components: the physical implementation of the antenna *figure 11(a)* and its frequency response in terms of return loss *figure 11(b)*. By evaluating the return loss is a essential for validating the antenna's real-world performance and confirming its suitability for targeted millimeter-wave 5G applications, specifically at the 28 GHz band. The return loss characteristics shown in *figure 11(b)*, are plotted over a frequency from 25 to 30 GHz. Two curves are presented, a red curve representing the simulated results obtained using full-wave electromagnetic simulation software (HFSS), and a blue curve representing to the measured results acquired using a calibrated VNA. The S_{11} parameter quantifies the amount of power reflected due to impedance mismatch and directly indicates how well the antenna is matched to the feeding transmission line. A return loss below -10 dB is generally considered acceptable and indicating that more than 90% of the incident power is delivered to the antenna and less than 10% is reflected. From the plot, it is observed that both simulated and measured curves exhibit a significant dip at approximately 28 GHz, confirming the resonant frequency of the antenna. The simulated return loss reaches a minimum of -32 dB, demonstrating excellent impedance matching and minimal reflected power. This demonstrates that the antenna is highly efficient at this resonant frequency and that the simulation model accurately captures the intended electromagnetic behavior. The measured return loss, although slightly higher at around -15dB, still falls within a very good range for practical 5G antenna designs. This measured value confirms that the fabricated prototype effectively resonates at the desired frequency and satisfies performance requirements.

The impedance bandwidth of the antenna is below -10 dB is another important performance metric. Both the simulated and measured results indicate a usable bandwidth of approximately 1GHz, centered around 28GHz. This wide bandwidth supports high data rates and low-latency transmission, making the antenna suitable for millimeter-wave 5G communication systems, where bandwidth demand is critical for enhanced mobile broadband and ultra-reliable low-latency communications (URLLC). However, a noticeable discrepancy exists between the simulated and measured S-parameters across the frequency range. Although the overall trend is similar, the measured curve shows a slightly higher return loss. These deviations are common in practical scenarios and can be arise from several real-world factors, including fabrication inaccuracies (slight variations in substrate thickness or copper trace dimensions), material inconsistencies (actual dielectric properties of the substrate may differ from the idealized values used in simulations) and connector or soldering imperfections during hardware assembly. Additionally, external influences such as nearby objects, environmental reflections, or test setup misalignment in the measurement setup may also impact the measured results. Despite these differences, the overall performance of the fabricated antenna remains robust and satisfactory.

FOREX Publication
Open Access | Rapid and quality publishing
International Journal of Electrical and Electronics Research (IJEER)
Case Study | Volume 14, Issue 01| Pages 10-17| e-ISSN: 2347-470X

Although the measured return loss does not reach the depth of the simulated one, it still indicates that the antenna is good impedance matched and efficient at the operating frequency. More importantly, the strong agreement in resonant frequency between simulation and measurement validate the proposed design methodology, comparison of the work with literature is represented in *table 2* and confirms the antenna's capability to operate reliably in the 28 GHz mm wave band.

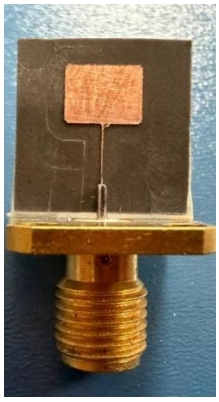

(a)

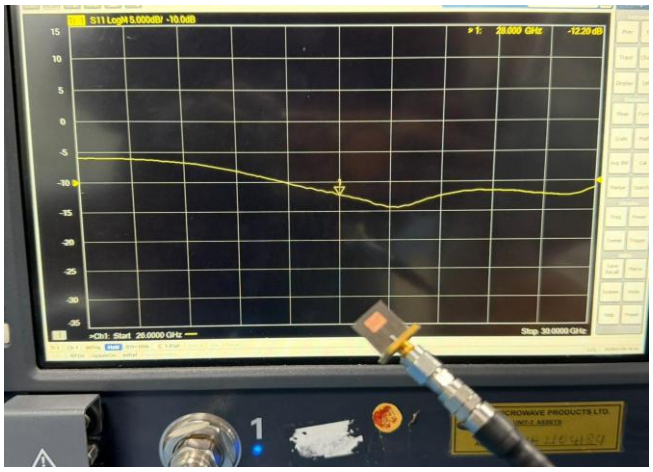

(b)

Figure 11. Proposed Balun feed truncated patch antenna (a) fabricated prototype (b) measured result using VNA

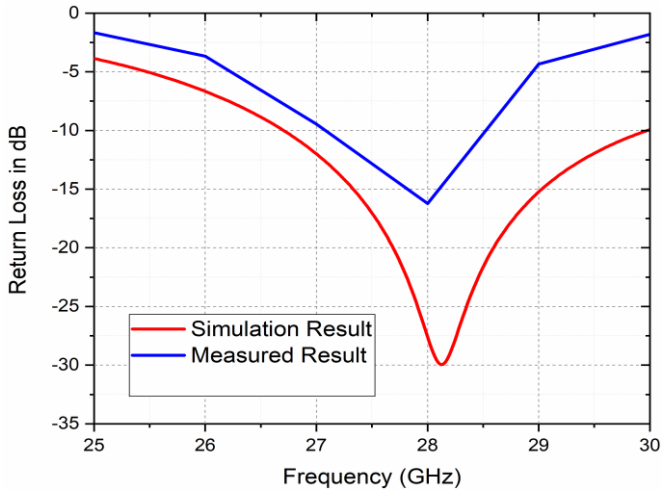

Figure 12. Return loss of Balun feed truncated patch antenna

Table 2. Comparison of the proposed antenna with literature

Ref. No	Size	Frequency (GHz)	Gain (dB)
[29]	$20 \times 20 \times 0.254$	28	8
[30]	$30 \times 35 \times 0.76$	28	8.3
[31]	$15 \times 19 \times 0.254$	24	7.41
Proposed antenna	$12 \times 12 \times 0.254$	28	6.9

5. CONCLUSION

This study comprehensively simulated and analyzed the key electromagnetic characteristics of 5G antenna geometrical configurations. The antenna parameters including S_{11} and VSWR exhibited consistent behavior across all the geometries. This consistency is attributed to the unchanged resonating surface and overall antenna dimensions, which ensured stable resonant frequencies throughout the designs. Despite the uniformity in resonant frequency, notable variations were observed in the magnitude of S_{11}, VSWR and antenna gain are summarized in *table 1*. These variations are primarily associate with modifications in the feed line geometry, which influence the impedance matching and electromagnetic field distribution across the patch. Specifically, reductions in S_{11} indicate improved impedance matching in certain configurations, while others showed slight degradation, likely due to abrupt or nonlinear feed transitions. The results and findings underscore the critical role of feed line design in optimizing antenna performance, even when the radiating elements remain constant or unchanged. As an extension of this work, future research should focus on fabricate physical geometries and perform experimental validation through key measurements such as S11, gain, and radiation pattern characterization. These evaluations provide a more understanding of the practical implications and performance reliability of the simulated antenna designs for real-world 5G applications.

Conflicts of Interest: Authors stated that no conflict of Interest.

REFERENCES

[1] B. O. Icmecz and C. Kurnaz, "High-Gain Dual-Band Microstrip Antenna for 5G mmWave Applications: Design, Optimization, and Experimental Validation," Applied Sciences, vol. 15, no. 7, p. 3993, 2025, doi: 10.3390/app15073993.

[2] A. Djouimaa and K. Bencherif, "Design of a Compact Circular Microstrip Patch Antenna for 5G Applications", Eng. Technol. Appl. Sci. Res., vol. 14, no. 4, pp. 16020–16024, Aug. 2024.

[3] S. R. Govindarajulu, R. Hokayem and E. A. Alwan, "A 60 GHz Millimeter-Wave Antenna Array for 3D Antenna-in-Package Applications," in IEEE Access, vol. 9, pp. 143307-143314, 2021, doi: 10.1109/ACCESS.2021.3121320.

[4] Tiang JJ, Alsekait DM, Khan I, Wang P-C and Madsen DØ (2024) Design of novel microstrip patch antenna for millimeter-wave B5G communications. Front. Mater. 11:1364159. doi: 10.3389/fmats.2024.1364159

[5] Al-Hiti, A.S., Ahmed, A.K., Mhmood, S.H. et al. Broadband and multiband millimeter wave microstrip patch antenna for 5G and 6G applications. J. Umm Al-Qura Univ. Eng.Archit. (2025). https://doi.org/10.1007/s43995-025-00161-w.

[6] Hua, Z., Gao, C., Peng, J., Fan, S. and Qian, Z., 2025. A Compact and Wideband Beam-Scanning Antenna Array Based on SICL Butler Matrix. Electronics, 14(4), p.757.

[7] A. Djouimaa and K. Bencherif, "Design of a Compact Circular Microstrip Patch Antenna for 5G Applications", Eng. Technol. Appl. Sci. Res., vol. 14, no. 4, pp. 16020–16024, Aug. 2024.

[8] Saraereh, O.A. (2021). A Novel Broadband Antenna Design for 5G Applications. Computers, Materials & Continua, 67(1), 1121–1136. https://doi.org/10.32604/cmc.2021.015066.

[9] Hua, Z.; Gao, C.; Peng, J.; Fan, S.; Qian, Z. A Compact and Wideband Beam-Scanning Antenna Array Based on SICL Butler Matrix. Electronics 2025, 14, 757. https://doi.org/10.3390/electronics14040757.

[10] Monti, Giuseppina, Laura Corchia, Egidio De Benedetto, and Luciano Tarricone. "Wearable logo-antenna for GPSGSM-based tracking systems." IET Microwaves, Antennas & Propagation 10, no. 12 (2016): 1332-1338.

[11] Shikder, Kawshik, and Farhadur Arifin" Extended UWB wearable logo textile antenna for body area network applications." In 2016 5thInternational Conference on Informatics, Electronics and Vision (ICIEV), pp. 484-489. IEEE, 2016.

[12] Ren, Wang, Li-Juan Zhang, and Shu-Wei Hu. "A novel ACPW-fed quad-band hybrid antenna for wireless applications." International Journal of Microwave and Wireless Technologies 10.4 (2018): 460-468.

[13] K. Kundu, A. Bhattacharya, F. H. Mohammed, and N. N. Pathak, "Design and Analysis of a Low-profile Microstrip Antenna for 5G Applications using AI-based PSO Approach", JTIT, vol. 93, no. 3, pp. 68–73, Sep. 2023, doi: 10.26636/jtit.2023.3.1368.

[14] Pozar, D. M. (2011). Microwave Engineering. Hoboken, NJ: Wiley.

[15] Balanis, C. A. (2016). Antenna Theory: Analysis and Design (4th ed.). Hoboken, NJ: Wiley.

[16] Kumar, G., & Ray, K. P. (2003). Broadband Microstrip Antennas. Norwood, MA: Artech House.

[17] Garg, R., Bhartia, P., Bahl, I., & Ittipiboon, A. (2001). Microstrip Antenna Design Handbook. Boston, MA: Artech House.

[18] Yang, F., & Rahmat-Samii, Y. (2009). Electromagnetic Band Gap Structures in Antenna Engineering. Cambridge, UK: Cambridge University Press.

[19] Álvarez Outerelo, D., Vázquez Alejos, A., García Sánchez, M., & Vera Isasa, M. (2015). Microstrip antenna for 5G broadband communications: Overview of design issues. 2015 IEEE International Symposium on Antennas and Propagation & USNC/URSI National Radio Science Meeting, 2443-2444.

[20] Muhammed Sheriff S., Obot Akaninyene B., and Udofia Kufre M., "Design and Optimization of Microstrip Antenna for 5G Wireless Applications using Genetic Algorithm", J. Eng. Res. Rep., vol. 26, no. 9, pp. 323–337, Sep. 2024.

[21] James, J. R., & Hall, P. S. (Eds.). (1989). Handbook of Microstrip Antennas. London, UK: Peter Peregrinus Ltd.

[22] Pozar, D. M. (1985). "Microstrip antennas with aperture coupling." Electronics Letters, 21(22), 1014-1016. https://doi.org/10.1049/el:19850702

[23] Wong, K. L. (2004). Compact and Broadband Microstrip Antennas. Hoboken, NJ: Wiley.

[24] El-Hakim, H., Mohamed, H.A. Synthesis of a Multiband Microstrip Patch Antenna for 5G Wireless Communications. J Infrared Milli Terahz Waves 44, 752–768 (2023). https://doi.org/10.1007/s10762-023-00937-y

[25] D. R. Basavaraju, R. Sukumar, "Design and Analysis of Microstrip Patch Antennas for Sub-6GHz 5G: A Comparative Study of Substrates and Feeding Techniques," SSRG International Journal of Electronics and Communication Engineering, vol. 11, no. 12, pp. 206-218, 2024.

[26] M. Nahas, "A High-Gain Dual-Band Slotted Microstrip Patch Antenna For 5G Cellular Mobile Phones", Eng. Technol. Appl. Sci. Res., vol. 14, no. 3, pp. 14504–14508, Jun. 2024.

[27] Anagh Sankar Das, Aditya Goel and Sangeeta Nakhate (2025), Investigating a Broadband Microstrip Patch Antenna that Demonstrates Enhanced Bandwidth for 5G-Based Applications. IJEER 13(3), 487-492. DOI: 10.37391/IJEER.130313.

[28] Jinan N. Shehab, Israa Hazem Ali, Huda I. Hamd (2025), Compact Folded T-Stub Microstrip Antenna with PIN Diode-Based Switching for Quad-Band Sub-6 GHz Wireless Systems. IJEER 13(4), 960-970. DOI: 10.37391/IJEER.130436.

[29] Jiang, H.; Si, L.; Hu, W.; Lv, X. A Symmetrical Dual-Beam Bowtie Antenna with Gain Enhancement Using Metamaterial for 5G MIMO Applications. IEEE Photonics J. 2019, 11, 1–9.

[30] Khalid, M., Iffat Naqvi, S., Hussain, N., Rahman, M., Fawad, Mirjavadi, S.S., Khan, M.J. and Amin, Y., "4-Port MIMO antenna with defected ground structure for 5G millimeter wave applications," *Electronics*, vol. *9*, p.71, 2020.

[31] Iqbal, A.; Basir, A.; Smida, A.; Mallat, N.K.; Elfergani, I.; Rodriguez, J.; Kim, S. Electromagnetic Bandgap Backed Millimeter-Wave MIMO Antenna for Wearable Applications. IEEE Access 2019, 7, 111135–111144.